GSICS Global Space-based Inter-Calibration System

Quarterly

Newsletter– Spring 2016 Issue

Volume 10 Number 1
2016
doi:10.7289/V5222RSK

Manik Bali, Editor
NCWCP College Park, MD, USA

CMA • CNES • EUMETSAT • IMD • ISRO • JAXA • JMA • KMA • NASA • NIST • NOAA • ROSHYDROMET • USGS • WMO

In This Issue

Image curtsey EO portal shows instruments of Jason family

LANDSAT-SRF

SELENE/SP

T-MODIS

MTSAT-2

Jason-3 Tandem Mission & Beyond: Maintaining Continuity of the Global Satellite Altimeter Record of Sea Level Rise

By Laury Miller, John Lillibridge and Eric Leuliette, NOAA

Sea level rise is often described as one of the greatest threats posed by global warming. Although the current global mean rate, 3.2 mm/year, may seem small, it is expected to grow over the next few decades with increased melting of Greenland and Antarctica ice sheets and ocean thermal expansion, possibly causing an overall rise of 1 meter or more by the end of the century.

A change of this magnitude would directly threaten several hundred million people worldwide currently living within 1 meter of mean high water, and put trillions of dollars of coastal infrastructure at risk (Nichols, 2011).

It is against this backdrop that Jason-3, the latest in a series of high precision satellite radar altimeters was launched on 17 January 2016. Jason-3 is a four-partner (National Oceanographic and Atmospheric Administration (NOAA), European Organization for the Exploitation of Meteorological Satellites (EUMETSAT), National Aeronautic and Space Administration (NASA), Centre National D'Etudes Spatiales (CNES)) mission designed to monitor sea surface height. Although used for near real-time ocean applications, including hurricane forecasting and oil spill monitoring, the primary function of this mission is to maintain continuity of the now more than two decade satellite climate record of global and regional sea level change.

Measuring sea level rise from space is challenging. It requires being able to detect global mean change with less than 1 mm error in any 1 year interval. To meet this exacting criterion over multiple missions, great care has been taken to maintain consistency in both the design and operation of the satellites. For example, Jason-3 and its two predecessors, Jason-1 and Jason-2, all employ the same bus and altimeter. For sampling continuity, each mission is flown in the same 10-day repeat orbit (1336 km altitude, 66° equatorial inclination) first occupied by TOPEX/Poseidon. Finally, to detect any bias or trend differences between missions, each new satellite is made to overlap with its predecessor, flying in close formation in what is called a Tandem Mission for at least 6 months. For example, Jason-3 is currently flying just 80 seconds behind Jason-2 on the same ground track. For an overview of the Jason-2 mission, the design of the satellite and the Jason-2 Tandem Mission see (Lambin et al. 2010; Leuliette and Scharroo 2010, and Lillibridge et al. 2012.)

In addition to the Tandem Mission comparison, Jason-3 is also calibrated with respect to two types of ground-based observations. Absolute calibrations are obtained from measurements made on the Harvest oil platform, off the California coast, by NASA and the Senetosa site on the island of Corsica, by CNES. Both sites are located on the 10-day Jason ground track and equipped with accurate, geo-located GPS receivers and tide gauges from which independent absolute biases are determined. A relative calibration is also obtained by comparison with the global network of tide gauges, many located near but not directly on the Jason ground track. This calibration is especially useful for determining any measurement drift, owing the large number (~70) of gauges available.

To illustrate the good performance of Jason-3 relative to Jason-2, Figure 1

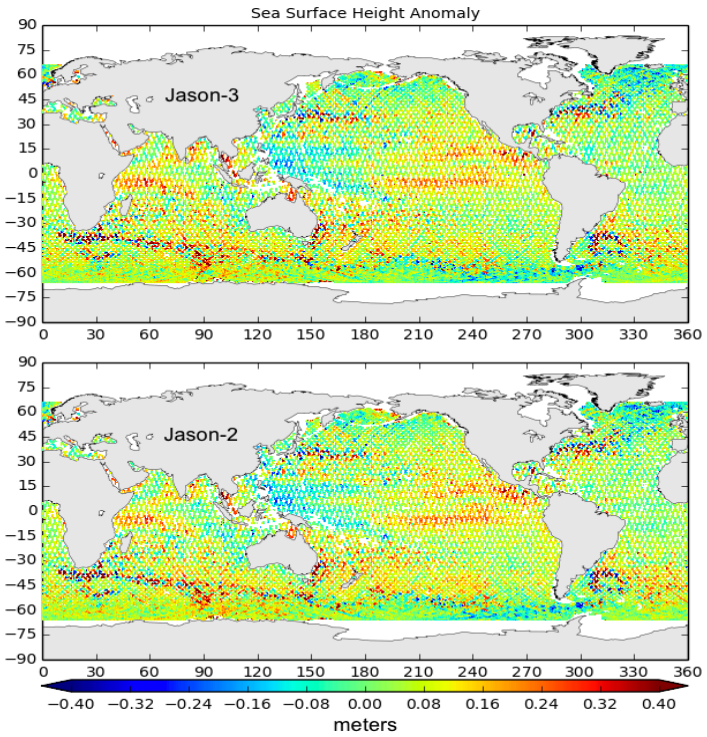

Figure1. Jason Tandem Mission Comparison: Upper plot shows first 10-day cycle (February 12-22, 2016) of bias adjusted Jason-3 sea level anomalies based on 3-5 hour latency Operational Geophysical Data Records (OGDRs). The lower plot shows same 10-day sample of Jason-2 observations. Each data point represents a 1-second along track average.

presents separate global sea level anomaly maps from the first 10-days (12-21 February 2016) of joint operation, less than one month after the launch of Jason-3. Although based on near real-time (2 to 3 hour latency) operational products (OGDRs), the two maps show the same large-scale patterns and details, including remnants of the current El Niño event in the equatorial Pacific, and small scale, eddy variability in the western boundary currents.

The Jason-3 observations in Figure 1 have been adjusted for a mean bias of 3.2 cm, currently under investigation. Although sizable, the bias is stable (rms of a few millimeters over multiple 10-day cycles) and not considered a problem for combining relative height observations. To illustrate this point, Figure 2 shows the multi-mission time series plot of global mean anomalies, where each mission has been adjusted to have zero bias relative to its predecessor based on a six month Tandem Mission overlap. The result is

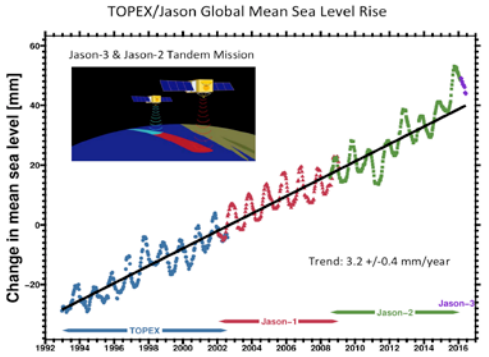

Figure 2. Global mean sea level rise over the past 23 years based on the combined TOPEX/Jason record. Plot shows the 6 month Tandem Missions used to correct bias differences between missions. Following the Tandem Missions, TOPEX/Poseidon continued to provide useful ocean observations for 3 more years and Jason-1 for 5 more years, but not in the reference orbit. Inset shows cartoon representation of Jason-2/OSTM and Jason-3 flying 80 seconds apart during the current Tandem Mission.

a remarkably consistent record of sea level rise over the past 23 years.

The least squares trend, 3.2 mm/year, is roughly 50% greater than the estimated rate during the past century from tide gauges, suggesting that global warming has already had an impact. Aside from the annual signal, other deviations reflecting the combined departures are related to large El Niño (1997-8, 2015-16) and La Niña (2010-2012) events.

Return to Page 1

The Jason-3 Tandem Mission will continue until September, 2016, when the satellite is expected to be declared operational and Jason-2 is moved to a separate 10-day ground track that effectively doubles the space/time sampling of the satellite pair. Although Jason-2 is now 8 years old, 3 years older than its design life of 5 years, the satellite is in excellent health and may continue to provide useful observations for a number of additional years before it becomes necessary to move it to an "end of life" orbit that protects the current reference orbit.

Although Jason-3 is just beginning its planned 5-year mission, preparations are already well underway for two follow-on missions designed for operational ocean applications as well as to maintain the climate sea level record to at least 2030. The first of these, Jason-CS-A/Sentinel-6A, has a planned launch date of 2020; the second, Jason-CS-B/Sentinel-6B, in 2026. (The Sentinel name identifies the mission as part of the European Unions' Copernicus Program). These satellites will employ a new bus based on CryoSat-2 and a new, high resolution Synthetic Aperture Radar (SAR) altimeter design that is backward compatible with Jason-3. Finally, both satellites will fly in the traditional TOPEX/Poseidon 10-day orbit, beginning with Tandem Missions, to ensure continuity of the climate sea level record

References

Lambin, J., R. Morrow, L. Fu, J.K. Willis, H. Bonekamp, J. Lillibridge, J. Perbos, G. Zarouche, P. Vaze, W. Bannoura, F. Parisot, E. Thouvenot, S. Coutin-Faye, E. Lindstrom, and M. Mignogno, (2010), "The OSTM/Jason-2 mission". *Marine Geodesy* 33(1): 4-25, doi: 10.1080/01490419.2010.491030

Leuliette, E.W. and R. Scharroo, (2010), "Integrating Jason-2 into a Multiple-Altimeter Climate Data Record", *Marine Geodesy*, 33(1): 504–517,doi:10.1080/01490419.2010.487795.

Lillibridge, J., H. Bonekamp , J. Willis, and P. Bonnefond, (2012), "Preface", *Marine Geodesy*, 35:sup1, 1-2, doi:10.1080/01490419.2012.721634

Nichols, R.J., (2011), "Planning for the impacts of sea level rise", *Oceanography*, 24(2): 144-157.

Discuss the Article

Spectral Response Characterization of the Landsat-8 Operational Land Imager

By Julia Barsi and Brian Markham, NASA

Introduction

The Landsat-8 satellite is the latest in the series of moderate resolution Earth imaging satellites in the Landsat program. The first Landsat was launched in 1972 and there has been at least one operational Landsat instrument on-orbit ever since. Landsat-8 was launched in 2013 with two instruments on board, the Operational Land Imager (OLI), and the Thermal Infrared Sensor (TIRS). The OLI is a pushbroom multispectral sensor with a 15° field of view and has nine spectral bands spanning the visible through the short-wave infrared (SWIR). The OLI focal plane is made up of 14 Focal Plane Modules (FPM), each with 494 individual detector elements per band.

Discussed here is the characterization of the relative spectral response (RSR) of the fully assembled OLI instrument as measured by the instrument vendor, Ball Aerospace & Technologies Corporation (BATC). More details on the complete spectral response characterization process can be found in Barsi, 2014.

For instrument level measurements, the OLI was placed in a thermal vacuum chamber and the light source (lamp and double monochromator) was outside the chamber. At the output slit of the monochromator, a beamsplitter sent part of the light to a monitor detector and part through a collimator to a window in the thermal vacuum chamber to the OLI (Figure 1). The OLI was pointed using ground support equipment (GSE) so that the collimated beam was projected onto 16 different locations for each band, one position at the center of each FPM and one each at the ends of the two extreme cross-field FPMs. The size of the beam was such that there was sufficient signal to characterize about 60 detectors at each location. At each location OLI data were collected, with the monochromator stepping through the OLI spectral bandpass in 1nm increments for the visible and near-infrared bands and at 2nm for the SWIR bands. The characterization was performed across a fixed wavelength range for each band that was designed to achieve responses down to at least 0.005 relative spectral response. Each OLI detector's digital response was offset corrected, normalized for temporally and spectrally dependent variations in the illuminating radiance and adjusted for the transmission of the path optics:

doi:10.7289/V5222RSK
Volume 10, No. 1, 2016

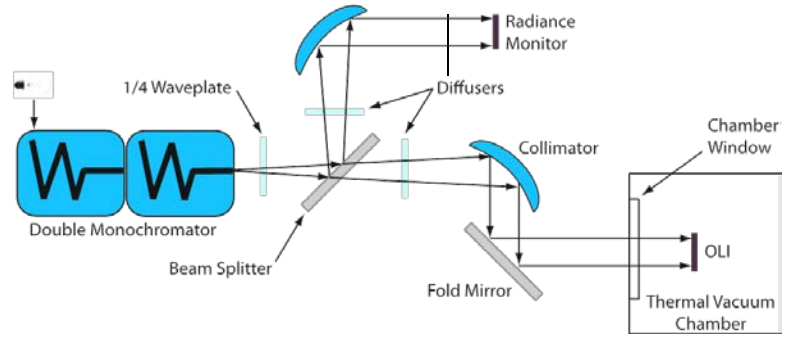

Figure 1. Schematic of spectral test setup for instrument level RSR measurements. The quarter waveplate was used to help ameliorate polarization induced by the monochromator; the diffusers were used to help ameliorate the jitter between the GSE and the OLI.

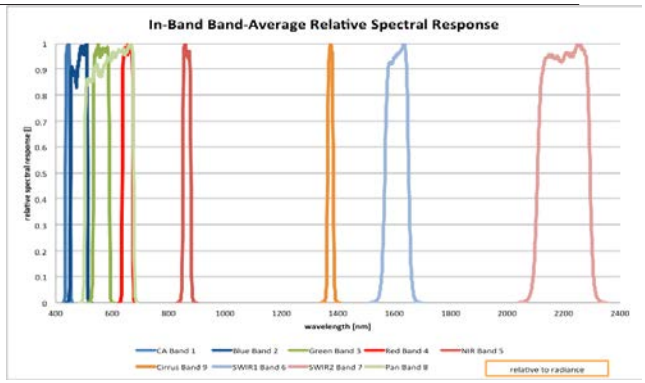

Figure 2. The band-average relative spectral responses of all bands of the OLI as determined from the instrument-level prelaunch tests.

$$S = \frac{(Q-Q_0)*R_m}{\tau_{OLIpath}}$$

where all quantities are per-wavelength and S is the derived spectral response, Q is the digital response of an OLI detector to the monochromator signal, Q_0 is the digital response of an OLI detector to no input radiance, R_m is the correction factor for the radiance output of the monochromator based on the monitor output and the monitor's radiometric calibration and $\tau_{OLIpath}$ is the transmission of the optical path between the beam splitter and the OLI. The spectral response is then normalized to unity at the peak response. The spectral response analysis was performed by both BATC and NASA/GSFC independently on the same data. The results presented here are from the GSFC analysis.

The test only directly measured about 14% of the OLI detectors in each band, but prior spectral measurements on the filters and detector arrays confirmed that there are no large spectral changes on a per-detector level, so it was sufficient to measure a sample of the detectors at the instrument level. The reported OLI RSRs are the average responses of the 14% of the detectors that were measured in each band. This means that the response does not actually reflect the response of any single detector.

Table 1. The center wavelength, edges and width of the OLI spectral bands as calculated from the 50% response points of the instrument-level test data.

Band	Bandwidth [nm]	Lower Edge Wavelength [nm]	Upper Edge Wavelength [nm]	Center Wavelength [nm]
Coastal Aerosol (CA)	15.98	434.97	450.95	442.96
Blue	60.04	452.02	512.06	482.04
Green	57.33	532.74	590.07	561.41
Red	37.47	635.85	673.32	654.59
Near Infrared (NIR)	28.25	850.54	878.79	864.67
SWIR1	84.72	1566.50	1651.22	1608.86
SWIR2	186.66	2107.40	2294.06	2200.73
Pan	172.40	503.30	675.70	589.50
Cirrus	20.39	1363.24	1383.63	1373.43

The most significant spectral differences across the focal plane are the result of filter-to-filter variations between FPMs. The green and red bands are the most uniform as all filters were from the same wafer. The other bands used filters from two or more different production batches and were less uniform (Figure 2). Much of the in-band low-amplitude high frequency structure is believed to be due to inadequate correction for the differences in the light path between the OLI and the monitor detector. For most applications this high frequency structure is not significant.
Additional tests were performed to detect response outside of the specified wavelength bandpass of every detector in each band. Those tests showed that only four out of the nearly 70000 detectors on the OLI had any out-of-band response above 10^{-3} within the required spectral range, and the integrated response beyond the 1% response points was 1% or less of the in-band response. Some spectral cross-talk was apparent in all the SWIR bands during prelaunch tests and, now on orbit, the cross-talk has been visible under very specific conditions in Cirrus band imagery (Barsi, 2014).

A summary of the OLI bands is listed in Table 1. The *Landsat web site* presents the per-wavelength, band-averaged, in-band relative spectral response, sampled at 1nm intervals along with the standard deviation of the measurements at each wavelength.

References

Barsi, J. et al., 2014, The Spectral Response of the Landsat-8 Operational Land Imager, *Remote Sens.* 2014, 6, 10232-10251; doi:10.3390/rs61010232

Discuss the Article

Return to Page 1

Lunar Calibration based on SELENE/SP Lunar Reflectance Model

By Toru Kouyama, Ryosuke Nakamura (AIST), Yasuhiro Yokota (Tsukuba Planet Science Group), Yoshiaki Ishihara (JAXA), Satoru Yamamoto and Tsuneo Matsunaga (NIES)

Introduction

Based on observation data from Spectral Profiler (SP) onboard SELENE, a Japanese Lunar Exploring orbiter operated from 2007 to 2009, the SP team has developed a new hyperspectral lunar reflectance model (Yokota et al., 2011) and its application scheme for conducting lunar calibration (Kouyama et al., 2016). Because the model covers the whole surface of the Moon and considers photometric properties (lunar surface reflectance and its dependences on incident, emission, and phase angles) with high spectral and spatial resolutions (6–8 nm wavelength intervals and 0.5° grid meshes in lunar latitude and longitude), it enables us to simulate disk-resolved Moon radiance images with any observation geometry in space.

Long-term radiometric calibration is indispensable for reliable and stable quality control of satellite data products. Since the Moon can be considered to be an extremely long-term photometrically stable object, more than one million years are needed for just 1% variation in the lunar surface reflectance (Kieffer, 1997), we can treat the Moon as an ideal target with known-brightness during mission lifetimes. There have been Earth observation missions that have adopted lunar calibration. During the SeaWIFS mission, the relative degradations of its multi-spectral sensors were confirmed with small uncertainties on the order of 0.1% (Eplee, et al., 2004). In addition, because the sensors can observe the Moon without any atmospheric absorption and scattering which could cause large uncertainties, especially in the spectral regions where strong water absorption exists, lunar calibration is an ideal method for hyperspectral radiometric calibration.

SELENE/SP lunar reflectance model

SP covered the visible (VIS: 512.6–1010.7 nm) and near infrared wavelength regions (NIR1: 883.5–1676.0 nm and NIR2: 1702.1–2578.9 nm) with a spectral sampling interval of 6 – 8 nm and 500 × 500 m footprint scale, and it observed whole lunar surface repeatedly with various solar incident and phase angles during the SELENE operation period (Matunaga et al., 2001; Yamamoto et al., 2011). Fortunately, SP did not show any degradation in its sensitivity during the mission (Yamamoto et al, 2011). Radiance conversion coefficients were obtained in preflight experiments.

Whole observation data are integrated into 0.5 x 0.5 degree grid in a longitude-latitude coordinate corresponding to ~8 arcsecond width seen from the Earth. The model provides radiance factor which corresponds to reflectance standardized with the specified solar incident angle (i), emission angle (e) and phase angle (α) of 30°, 0° and 30°, respectively. Figure 1 shows the radiance factor map of the SP model at 752.8 nm, and an example of the radiance factor spectrum at a grid point of longitude 0° and latitude 0°.

Using the radiance factor, we can simulate the instantaneous lunar surface reflectance at each grid point when we provide i, e and α. The radiance factor r_{sim} at a grid point is estimated from

$$r_{sim}(\lambda,i,e,\alpha) = r_{corr}(\lambda,30°,0°,30°)\frac{X_L(i,e,\alpha)}{X_L(30°,0°,30°)}\frac{f(\alpha)}{f(30°)} \quad \text{.....(1)}$$

where λ represents the wavelength and r_{corr} is the radiance factor provided in the SP model. X_L is the linear combination of the Lommel-Seeliger and Lambert scattering laws and f is an empirical function for describing the phase angle dependency the SP team measured (see Yokota et al., 2011). Then the simulated lunar surface radiance R_{sp} (W m^{-2} μm^{-1} sr^{-1}) can be obtained by multiplying r_{sim} by the solar irradiance and correcting for the distance between the Sun and the Moon,

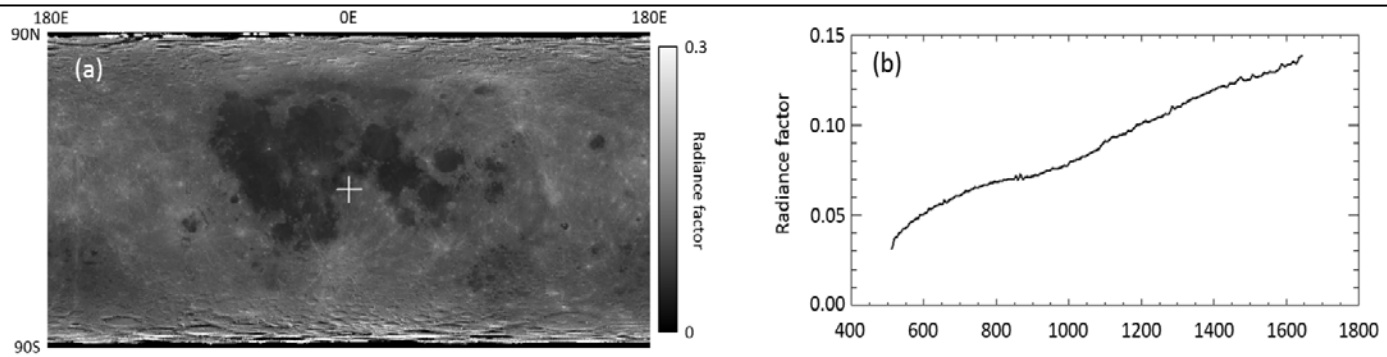

Figure 1. (a) Radiance factor map on a 0.5° × 0.5° grid at 752.8 nm. (b) Spectrum of radiance factor at (0°, 0°) latitude and longitude (marked with "+" in (a)). (after Yokota et al., 2011)

Return to Page 1

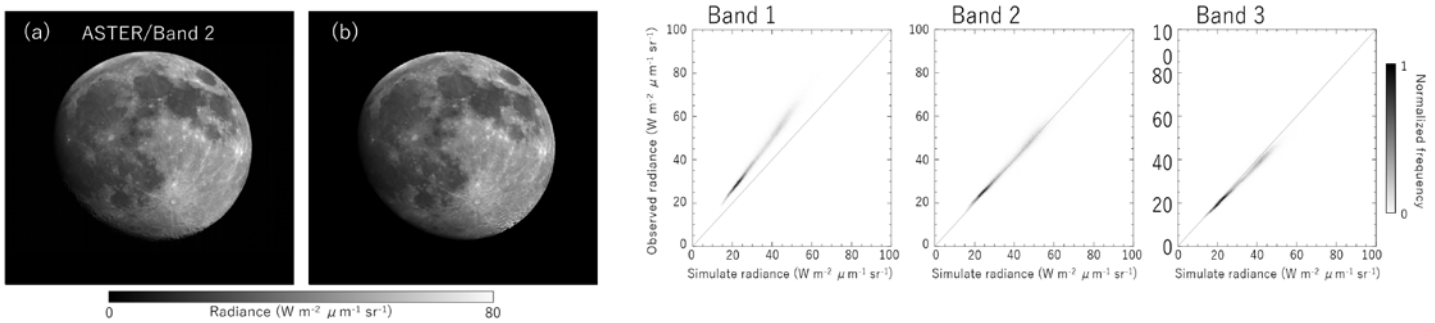

Figure 2. An example of a pair of (a) observed and (b) simulated Moon images, and (right panel) frequency distributions from comparisons of the observed and the simulated radiances of the Moon. The observed Moon image was taken by ASTER (Band 2) on April 14, 2003.

$$R_{SP}(\lambda) = r_{sim}(\lambda, i, e, \alpha) \cdot \frac{I_{Sun}(\lambda)}{\pi} \cdot \left(\frac{D}{1AU}\right)^{-2} \quad \text{....(2)}$$

where I_{Sun} is the solar irradiance (W m^{-2} μm^{-1}) at a distance 1 AU and D represents the distance in units of AU.

Performance of SP model

From these equations, we can draw a simulated Lunar radiance image once we provide i, e, and α at each pixel of a considered detector. Figure 2 shows a simulation example of a pair of observed [Advanced Spaceborne Thermal Emission and Reflection radiometer (ASTER) Band 2: 630-690 nm] and simulated Moon images. Figure 2 also shows a frequency distribution of the radiance from pixel-based comparison, showing good consistency between both images. Because the correlation coefficients exceed 0.99 for all ASTER VNIR bands (Band 1, 2, and 3), we have considered that the simulated Moon image accurately describes the Moon's features (brightness patterns) seen in observation.

However, unlike the high correlations, it has been confirmed that absolute magnitude of simulated radiance shows some bias which indicates the simulated radiance is ~30% darker than the observed radiance in a shorter wavelength and several percent brighter in a longer wavelength from the comparison with ASTER data. One possible reason for these discrepancies is SP calibration issue for measuring absolute magnitude of radiance in which SP tended to provide darker brightness in shorter wavelength region compared with other sensors, according to a study investigating consistency among many sensors observing lunar surface (Ohtake et al., 2013). In contrast, the standard deviations of all bands are less than 5%, which indicates that the relative magnitude of the observed brightness to the simulated brightness can be determined with small uncertainty (< 5%) at each pixel. We have expected that the SP model is useful for evaluating the relative degradation of sensors with small uncertainty (several percent for pixel-based calibration and more accurate evaluation could be expected for mean sensor degradation), considering that observed lunar radiance from different observations can be compared via the simulated lunar radiance.

Challenges for improving the absolute accuracy of SP model have been identified and addressed. We have confirmed the large discrepancy seen in the comparison of absolute radiances in Band 1 is reduced from 30% to several percent by using a correction coefficient deduced from a comparison between SP model and another lunar reflectance model developed from the RObotic Lunar Observatory (ROLO), a ground-based telescopic system (Kieffer and Stone, 2005).

Collaboration with other lunar reflectance/irradiance models, such as ROLO, GIRO (GSICS Implementation of the ROLO model), and Miller-Turner lunar irradiance model (MT2009, Miller and Turner, 2009) should provide a good opportunity to ensure the reliability of SP model and its contribution to the lunar calibration activities.

References

Eplee R. E., et al., SeaWiFS Lunar Calibration Methodology after Six Years on Orbit, Proc. SPIE—Earth Observing Systems IX, 5542, 1-13, 2004.

Kieffer, H.H. and Stone, T.C., The spectral irradiance of the Moon, Astron. J., 129, 2887–2901, 2005.

Kouyama et al., Development of an application scheme for the SELENE/SP lunar reflectance model for radiometric calibration of hyperspectral and multispectral sensors, Planet. Space Sci., 124, 76-83, 2016.

Matsunaga, T., et al., Development of a visible and near infrared spectrometer for Selenological and Engineering Explorer (SELENE). Proc. SPIE Int. Soc. Opt. Eng., 4151, 32–39, 2001.

Ohtake, M., et al., One Moon, Many Measurements 3: Spectral reflectance, Icarus, 226, 364-374, 2013.

Yamamoto et al., Preflight and In-Flight Calibration of the Spectral Profiler on Board SELENE (Kaguya), IEEE Trans. on Geoscience and Remote Sensing, 49, 4660-4676, 2011.

Yokota Y., et al., Lunar photometric properties at wavelengths 0.5-1.6 μm acquired by SELENE Spectral Profiler and their dependency on local albedo and latitudinal zones, Icarus, 215, 639-660, 2011.

Discuss the Article

Return to Page 1

doi:10.7289/V5222RSK
GSICS Quarterly: Spring Issue 2016 Volume 10, No. 1, 2016

Electronic Crosstalk Contamination in T-MODIS: An Overview

By Sriharsha Madhavan and Junqiang Sun, NOAA

Satellite data products from heritage sensors, such as the MODerate Resolution Imaging Spectroradiometer (MODIS), are critical for the long term Climate Data Record (CDR). Further, the CDRs based of MODIS are a vital bridge for the Environmental Data Records derived from the current and next generation sensors such as the Suomi Visible Infrared Radiometer Suite (S-VIIRS). The fidelity of these records depends greatly on the accuracy of the sensor calibration. To achieve high accuracy, instruments, such as MODIS, are bestowed with several on board calibrator sources that are traceable to good ground references.

Terra-MODIS (T-MODIS), a premier heritage instrument in the NASA's Earth Observing Systems, celebrated its 15-year anniversary on December 18 2014 marking a grand success of the NASA's EOS mission. Spectral bands long ward of 3.7 µm are referred to as Thermal Emissive Bands (TEBs). The TEBs are housed in cooled environment where the Focal Plane Assembly (FPA) is maintained at a temperature of 83 K. This is done in order to ensure a higher Signal-to-Noise Ratio (SNR). All the TEB detectors are located on the cooled FPA, are split into the Short and Mid wave Infrared (SMIR) and the LWIR planes respectively. Based on the instrument gain and noise trends, detectors of bands 27-30 have shown large radiometric gain drifts, larger than 12% as of mid-2015. The performance in terms of noise given by NEdT has also significantly increased since 2010. These have been chiefly attributed to the electronic crosstalk contamination and are reported in various articles, e.g., Sun, Madhavan and Wang 2016.

In this newsletter article, the electronic crosstalk contamination in band 30 will be discussed as a prime example due to the following reasons. Firstly, the crosstalk magnitude is the highest in comparison to the other bands. The problem is quite complex for band 30 because not only the linear calibration term is significantly affected but the higher order calibration term is also. Together, the effect has caused approximately 2.5 to 3 K long term drifts along with significant detector-to-detector mismatches. Electronic crosstalk is a phenomenon that contains the induction of electronic signals from neighboring detectors on the same FPA. In the case of MODIS, the electronic detectors are stacked in an array like formation. This means the signals interference amongst themselves would manifest itself as a striping artifact or a ghosting type of pattern depending on the signal levels of the crosstalking bands and the time integration of the recieving signal. The moon surface serves as a viable source to characterize the electronic crosstalk in MODIS. Figure 1 displays a three dimensional rendition of the moon surface for band 30 detector 1 obtained for two time periods (2000, 2012). The x axis is frames of the moon acquistion as seen in the Space View port, while the y axis gives the observations in along scan direction. The z axis shows primarily the moon signal which is seen as a cylindrical structure with a saturated plateau. For illustration purposes of the crosstalk signal, the z axis is intentionally truncated to 200 counts. Typically, the lunar signal is quite high close to 4000 counts. From Figure 1a and 1b it can be seen that for band 30 detector 1, the crosstalk impact is positive early in life and is then negative later in the mission.

The electronic crosstalk correction algorithm is modeled as a linear function with the effective crosstalk coefficient computed as a band-averaged estimate from the three sending bands 27-29. The crosstalk components are a function based as sum of products from the three sending bands. In terms of equation, they are given as Equation (1) below:

$$dn_{B_r D_r}(F) = d^{msr}_{B_r D_r}(F) - \sum_{B_s} C(B_r, D_r, B_s)\left\langle dn^{msr}_{B_s D_s}(F + \Delta F_{rs})\right\rangle_{D_s}$$

…… (1)

where *dn* is the background subtracted digital response, *B*, *D* refer to band and detector, *r* and *s* correspond to the receiving and sending bands, *msr* indicates that the *dn* is the response with crosstalk correction, $C(B_r,D_r,B_s)$ is the sending band averaged crosstalk coefficient for the crosstalk from band B_s to band B_r with the detector D_r, F is the frame number along the scan, and ΔF_{rs} is frame shift between bands B_s and B_r.

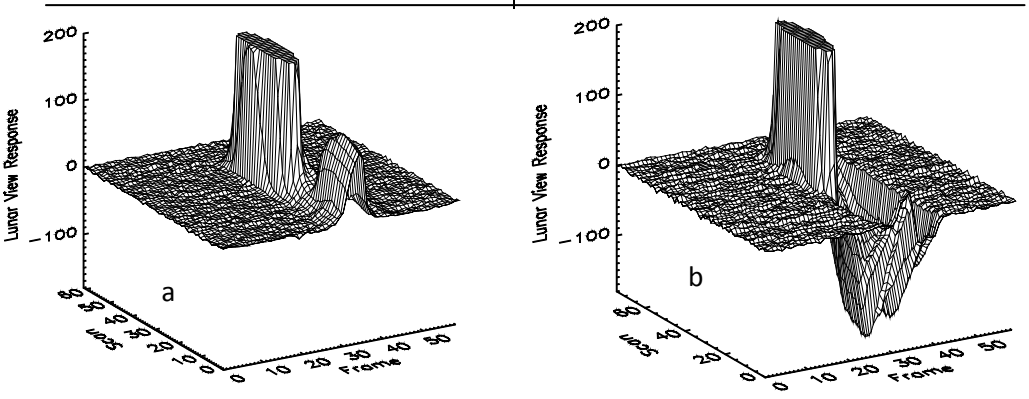

Figure 1. Lunar Surface for T-MODS band 30 detector 1: a. December, 2000; b. December, 2012.

Return to Page 1

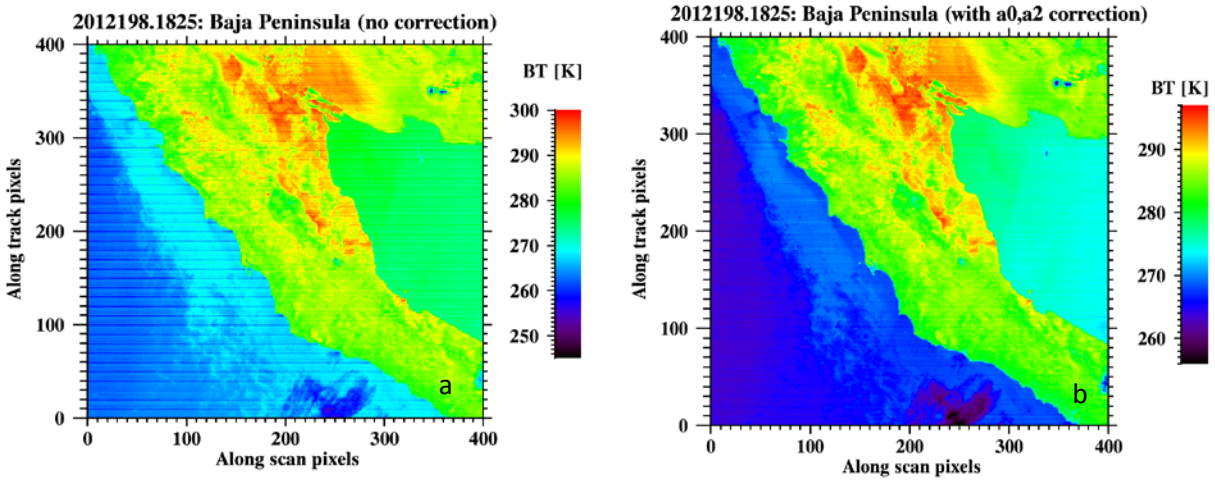

Figure 2. Crosstalk induced striping and removal in BT of Terra MODIS band 30 at Baja peninsula in 2012: a. before crosstalk correction; b. with crosstalk correction applied to all calibration terms, and Earth View

With the derived crosstalk coefficients using Eq. (1), the correction is applied at two points in the Level1 B (i.e. radiometric correction) calibration. First the application of the *dn* correction is made to the on-board Blackbody responses and then to the Earth View responses. Figure 2a shows the Baja California region from 2012 in terms of retrieved Brightness Temperature (BT) of band 30 before crosstalk correction is applied. It is quite evident that the detector mismatches in response have manifested into striping noise. Figure 2b, shows the same Baja Image after the correction is applied to all the calibration terms. The correction not only removes the striping noise but significantly increases the visual appeal of the complete corrected image. With the corrections applied to the calibration terms and EV radiance, the striping noise is reduced to within 0.5 K. Thus the qualitative and quantitative study using Baja imagery indicates that the crosstalk correction algorithm described by Eq. 1 is very good and accurate. Further analysis using Earth View sites such as the Pacific Ocean and Libya 1 desert showed a removal of the long-term radiometric drift of approximately 2 K. The long term corrected trends were essentially flat as is expected in most geophysical variable measurements. The results presented here warrant a strong recommendation that the crosstalk correction be applied to the LWIR bands 27-30 in future MODIS collection.

References

J. Sun, S. Madhavan, M. Wang, Investigation and Mitigation of the Crosstalk Effect in Terra MODIS Band 30. Remote Sens. 2016, 8(3), 249; doi:10.3390/rs8030249.

Discuss the Article

How World Metrology is Organised

By Emma Woolliams, National Physical Laboratory, UK

The metrological community maintains the International System of Units (SI) and associated derived units, and ensures that these are stable over centuries, even while also improving, as technology advances. They must also remain uniform worldwide and independent of the method used to realise the unit. These concepts: century-long stability and independence of both measurement method and country of origin are the same aims that satellite-derived Earth observation (EO) needs to meet the requirements of long-term climate trend analysis. It is therefore natural that there is an increasing dialogue between metrology and EO. A first step to encourage the adoption of metrological methods in the EO community was the development of the Quality Assurance Framework for Earth Observation (QA4EO: www.qa4eo.org) by CEOS. This paper discusses some of the principles of metrology as background information to that dialogue.

Metrology is the science of measurement, encompassing empirical and theoretical determinations of measurement uncertainty. Arguably, metrology became a recognised discipline in 1875, when representatives of 17 nations signed the *Convention du Mètre* (Metre Convention).

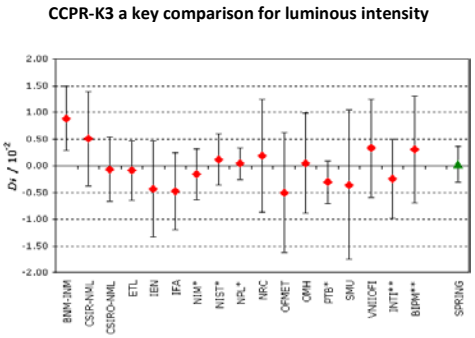

Figure 1. Example Key Comparison Results. Here for Luminous Intensity. See the BIPM Key Comparison Database (http://kcdb.bipm.org) for more examples.

This convention founded the *Bureau International des Poids et Mesures* (BIPM: International Bureau of Weights and Measures) and an organisational structure for member governments to co-operate in all matters relating to units of measurement. The convention (modified in 1921) remains the basis of the international measurement system and has now been signed by 56 nations. The convention constituted BIPM as a scientific body, researching physical standards and the determination of physical constants. Such research continues both at the BIPM itself and at the National Metrology Institutes (NMIs) of member nations.

This metrology community is responsible for the International System of Units (*Système International d'Unités*, SI) which provides the foundation for measurement around seven base units and a system of coherent derived units. 'Coherent' here means that there is no scaling factor when combining units: an electrical joule is equivalent to a mechanical joule, for example, and the method of measurement does not affect the determined quantity.

There are three key concepts underpinning how the desired stability and consistency of these units is achieved: uncertainty analysis, traceability and comparisons. Uncertainty analysis is the systematic review of all sources of uncertainty associated with a particular measurement and the formal propagation of uncertainties through methods defined by the Guide to the Expression of Uncertainty in Measurement (GUM). Traceability is the concept that links all metrological measurement to the SI through a series of calibrations or comparisons. Each step in this traceability chain has rigorous uncertainty analysis, usually peer reviewed or audited and always documented. Comparisons are the process of validating an uncertainty budget by comparing the measurement of artefacts by different laboratories.

NMIs have always used comparisons for scientific purposes, to test their methods and especially their uncertainty budgets. In the early stages of research these scientific comparisons show up the unknown unknowns – the differences between participants that are not (yet) considered in the uncertainty budgets. As a field matures and the technical approaches move from research to operational measurement services, comparisons show increasing agreement between participants. At this point the role of comparisons changes from research into auditing and peer review.

This second purpose was formalised in 1999 by the signing of the Mutual Recognition Arrangement (MRA) by the world's NMIs. The MRA says that 'within an appropriate degree of equivalence' the results of one NMI can be considered equivalent to the results of another NMI. In practice this enables world trade and the use of artefacts and instruments calibrated in another country. The MRA works because NMIs regularly review each other's calibration and measurement capabilities through a combination of formal peer review and auditing and through formal 'key comparisons' that compare the measurement capability of laboratories – both at the international level (by a handful of laboratories with, generally, the lowest uncertainties) and at the regional level (e.g. within Europe or within Asia-Pacific).

The formal key comparisons are run with strict guidelines and are always blind comparisons (only one 'pilot' laboratory has access to the results before they are published). There is ongoing discussion about the best ways of analysing such comparisons, and in particular about the choice of the Key Comparison Reference Value (KCRV) against which all participants are compared. In very mature fields, where the differences between the measured values of the different participants and the KCRV are consistent with uncertainties, the most common KCRV is the weighted mean of the results of the different laboratories. In fields where there is more spread, this may not be the appropriate choice and alternatives (including 'weighted mean with cut-off' which limits the weight assigned to the laboratories with the lowest uncertainties, or simply using a median value) are considered.
These key ideas of metrology – rigorous uncertainty analysis, formal traceability and the use of comparisons both for scientific research and for formal auditing – are what has ensured the stability of the international measurement system. It is now 140 years since the signing of the Metre Convention, and 55 years since the SI was established. As EO increasingly moves into research of the climate, where similar timescales are of interest, it is worth considering how these ideas can be integrated with the existing approaches to uncertainty analysis in EO.

Discuss the Article

News in this Quarter

Highlights on 2016 Annual GRWG/GDWG Meeting

By Manik Bali, Lawrence E Flynn (NOAA), Tim Hewison (EUMETSAT) , Doheyong Kim (KMA), Peter Miu (EUMETSAT) and Masaya Takahashi (JMA)

This year's meeting of the GRWG and GDWG was hosted by JAXA and JMA, Tsukuba, Japan on 29 Feb - 04 March 2015. Members from JAXA, JMA, NASA, NOAA, CMA, CNES, KMA, USGS and EUMETSAT, and observers from AIST, Ewha Womans University, KIOST and NIES attended the meeting in person while, ISRO presented remotely.
After an impressive opening ceremony, including welcome speeches by Chu Ishida (JAXA) and Yoshiteru Kitamura (JMA) the meeting started with a Mini Conference. Dave Doelling started the technical presentations by describing the CLARREO Pathfinder mission, which should provide SI traceable radiances that could be used as in-orbit reference for calibration. Talks on FIDUCEO (By Rob Robelling), Lunar Calibration (By Scott, Xiangqian Wu, and Toru Kouyama) initiated discussions on vital current and future GSICS deliverables and products.

The Mini Conference was also an opportunity for the hosts, JAXA and JMA, to showcase their missions, namely the excellent results and plans for Himawari-8, GCOM-C/-W, GOSAT /GOSAT-2, ALOS/ALOS-2, TRMM and GPM Radars.

The Mini Conference was followed by the plenary session the next day, featuring GCC, GDWG and GRWG subgroup reports and agency reports to update members about their recent GSICS activities. The minutes are available at Meeting minutes and the talks can be downloaded from http://gsics.atmos.umd.edu/bin/view/Development/20160229.

GSICS Coordination Center (GCC)

The GCC is at the cross roads of all the GSICS activities. Larry Flynn (GCC Director) and Manik Bali (Deputy Director) led the GCC discussions. They reported that the EUMETSAT, MSG 2/3 – IASI-A cross calibration product has attained the Operational status in the GPPA. This is the first time that a GSICS product has attained the highest maturity level in GPPA. They also reported the status of rest of GSICS products (4 in pre-operational and 27 products in demonstration phase of GPPA). The GCC Director concluded by inviting members to the GSICS Users Workshop, 2016 that will take place an August 11 at NCWCP in College Park MD USA.
Larry and Manik touched upon several topics vital to GSICS activities. These included products categorization, product acceptance and promotion for newly submitted GSICS products, and selecting reference instruments. It is envisaged the new categorization would lead to a range of products and resources coming into the GSICS fold and made available to the calibration community. These include intermediate inter-comparison data, instrument health monitoring, models and data sets. The proposal is up for GSICS Executive Panel consideration.
Manik gave a summary of the user requirements survey and sought feedback on GSICS newsletter. He reported that in the past year the GSICS Newsletter carried over 25 Research Articles, over 15 Topics of News in which over 70 researchers contributed as authors or coauthors.

GSICS Research Working Group

The Research Working Group sessions had 42 presentations on topics including GEO-ring data analysis, prime GSICS reference, GEO-LEO IR progress, DCC demonstration products, and lunar calibration.
The GEO-ring is the application of the GSICS corrections to calibrate the IR channels of the global array of GEO imagers to be consistent with a single reference instrument. The dataset for GEO ring will be for two proposed dates (1 and 20 March 2014) with Full Disk images taken every 3 hours from the participating instruments flown by EUMETSAT, NOAA, JMA, KMA, CMA and ISRO. These data will be provided to the SCOPE-CM IOGEO project to test their homogenization and demonstrate global L2 product retrievals.
Another important topic is the need for an *anchor* or primary comparison reference. Tim introduced the method to move from one reference to another or to make use of multiple references - either by directly blending them as a weighted average, or by adjusting them to the anchor reference first. He submitted the working paper on this subject to CGMS-44 in June 2016.

Improving the reference standard for lunar calibration was discussed. Tom Stone suggested acquiring both high-accuracy, SI-traceable ground-based and space-based measurements to establish an absolute lunar reference standard. He also presented CGMS working paper with the title of "Requirements for an absolute lunar calibration reference for solar band radiometer instruments".

Return to Page 1

Participants of the GSICS Annual GRWD GDWG Meeting at Tsukuba (JAXA), Japan

NASA led the GSICS DCC calibration discussion encouraging GSICS members to submit demonstration products, and to write GSICS DCC algorithm papers with input from all GPRCs.

Other sessions concentrated on the further development of demonstration products based on the Deep Convective Cloud inter-calibration method, and planned ways to merge these results with those from developing lunar inter-calibration methods.

GSICS Data Working Group

In the Data Working Group sessions, 19 topics such as creating a repository for source codes, developing metadata standards for VIS/NIR GSICS Products and updates of the GSICS THREDDS server configuration were discussed.

One of the most important collaboration issues discussed is the mirroring of GSICS products across the GSICS collaboration servers (EUMETSAT, NOAA and CMA). This is an urgent issue because SEVIRI vs. IASI IR inter-calibration products are now available as Operational Products that are expected to be available on all GSICS collaboration server.

NOAA (Manik Bali) has established a GSICS product mirror site. This site can be accessed at http://www.star.nesdis.noaa.gov/smcd/GSICS_PC_MIRROR/gsics.eumetsat.int/thredds/catalog. In addition to the regular GSICS product catalog all GSICS products can also be downloaded from this website. A new directory structure separating PRIME GSICS products from individual references products was also discussed and adopted.

Jordan Yao from NOAA reported that he has ported the GSICS Wiki from NOAA to a University of Maryland web server. Further work is continuing to correct the http links. The GDWG also gave input to the GCC on action tracking tool that GCC is maintaining. The new wiki location can be accessed at http://gsics.atmos.umd.edu/wiki/Home

In the 2016 meeting, two concepts were discussed to improve the efficiency in tracking GSICS actions. The first was a simple solution to update the existing Actions Tracking developed in the GSICS Wiki to offer sort and possibly, a filter and email functionality to improve usability. A more sophisticated action tracking process for alerting open actions was also presented with an optional automation design. Both these concepts will be presented to the GSICS Executive Panel for discussion.

To support the GRWG lunar calibration activities, the group invited GRWG colleagues of EUMETSAT, USGS, CNES and AIST to investigate how to share with developers and users the GSICS Implementation of the ROLO (GIRO) codes and the GSICS Lunar Observation Dataset (GLOD).

Based on the attributes of the how the system is to be used, a simple proposal was made and accepted to send the deliverables to users directly after manual registration. It was also proposed that user support can be provided through the GSICS wiki by using a Forum or Frequently Asked Question page. EUMETSAT will continue to lead this activity.

Discuss the Article

Return to Page 1

MTSAT -2 Stops Data Distribution, Himawari-8 Takes Over its Role

By Masaya Takahashi, JMA and Manik Bali, NOAA

On 24 March 2016 the MTSAT-2 formally stopped distributing data. Its role has now been taken over by the Himawari-8 which started operation on 7 July 2015. The MTSAT-2 continues to act as a backup to the Himawari-8 until Himawari-9 is placed in on-orbit storage.

With the cessation of MTSAT-2 product distribution, the production of MTSAT-2 – IASI-A and MTSAT-2 – AIRS inter-calibration GSICS product developed by JMA has also stopped. AIRS and IASI-A were used routinely to monitor MTSAT-2 in Near Real Time and Reanalysis Mode. Analysis of GSICS inter-calibration product has revealed that the MTSAT-2 has been stable during the time of its operations even though some channels have diurnal calibration biases.

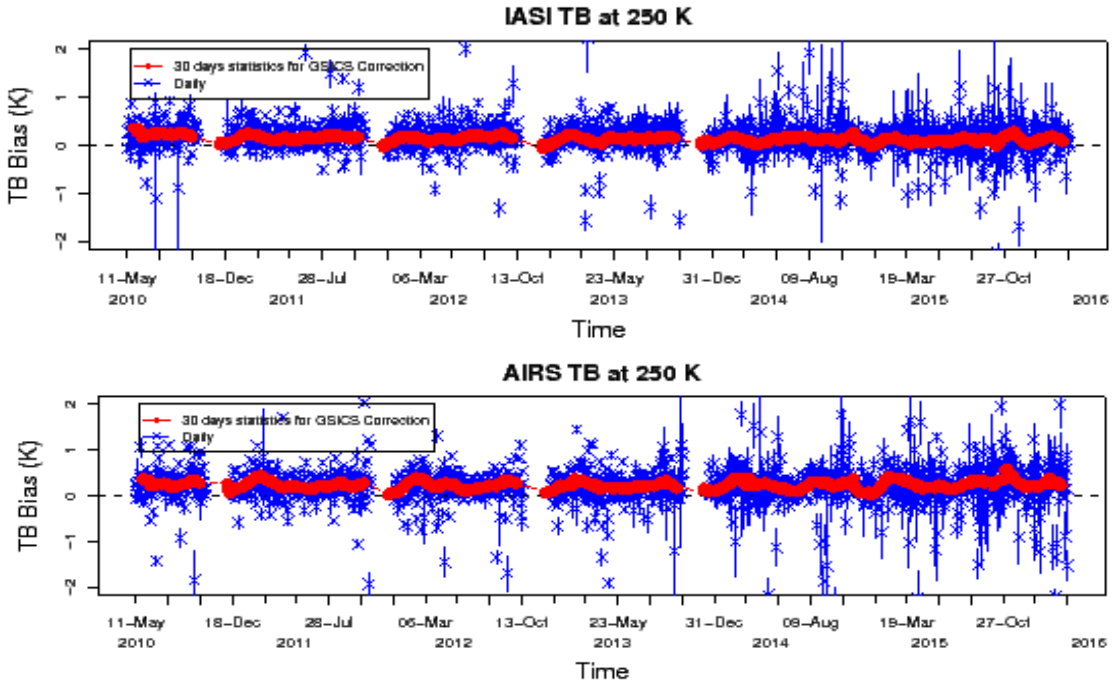

Figure 1: Shows the MTSAT-2 – IASI-A bias (top) and MTSAT-2 – AIRS bias (bottom) for 12µm at 250K. MTSAT-2 has been stable

8th GRUAN Implementation and Coordination Meeting (ICM-8)

By Tony Reale (NOAA), Peter Thorne (Maynooth University) and Bomin Sun (NOAA)

The Global Climate Observing System (GCOS) Reference Upper Air Network (GRUAN) (http://www.dwd.org) is a reference observing network designed to provide long-term, climate quality data records from the surface, troposphere and stratosphere (Bodeker et.al, 2016). Reference observations are calibrated through an unbroken traceability chain to SI or community standards and the uncertainty in each step in the chain is fully characterized, meaning the resulting estimates can be used with high confidence that the true measurement exists within the interval (Immler et al., 2010). The primary objectives of GRUAN include monitoring climate trends, constraining and calibrating data from other more spatially extensive observing systems such as satellites and the current radiosonde network and fully characterizing the properties of the atmospheric column above a given site. GRUAN has grown from a call in the first GCOS Implementation Plan back in the early 2000s to a network of over 20 sites (and growing) either formally certified or in various stages of the certification process. These are shown in Figure 1. GRUAN is ultimately envisioned as a global network of 30-40 sites.

The 8th GRUAN Implementation and Coordination Meeting (ICM-8) was held in Boulder Colorado from 25 to 29 April, 2016; this was also the location of the original meeting that led to the

Return to Page 1

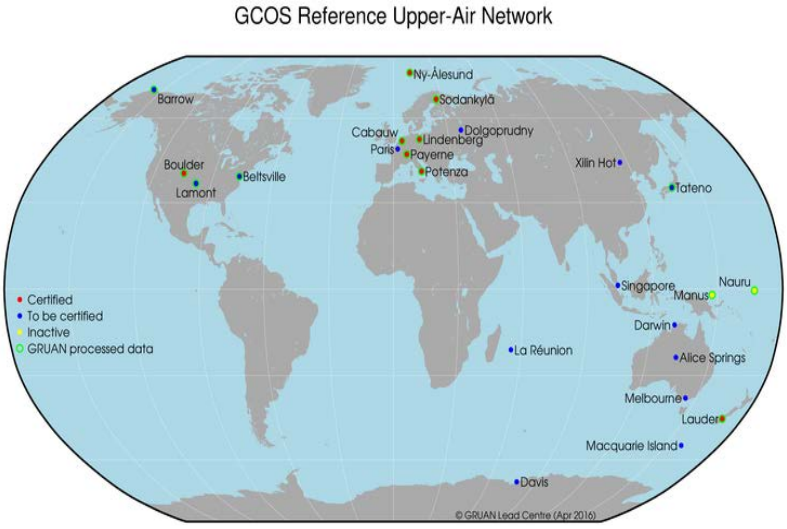

Figure 1: Location and status of GRUAN sites as of ICM-8, April 2016.

formation of GRUAN back in 2005. ICM-8 hosted over sixty international scientists and addressed a wide variety of topic areas including strategic planning, change management, development and validation of new data streams, documentation, metadata, synergy with observations from other networks, and the potential impact on our current understanding of climate change processes.

A focus for ICM-8 was management of the change from the Vaisala RS92 to RS41 radiosondes across GRUAN.The RS92 has been the main reference radiosonde processed for GRUAN but will no longer be manufactured after September 2017, when it will be replaced by the RS41.

Radiosondes comprise the primary source of high vertical resolution profiles of temperature, pressure and humidity from the surface to the middle stratosphere at GRUAN sites and are also critical for calibrating and characterizing other ancillary measurements available at GRUAN sites. Constructing a best estimate of the state of the atmospheric column and its uncertainty at high spatial and temporal resolution is achieved by combining the available ancillary and radiosonde profiles, each with known spatial and temporal attributes and traceable quantified uncertainties. It is therefore crucial to have a clear understanding of the RS92 and RS41 measurement and uncertainty differences to ensure the integrity of the long-term GRUAN climate record at each site.

Another point of discussion at ICM-8 was the need to expand the GRUAN network for a more balanced global representation. Figure 1 shows a preponderance of sites over Europe and the United States with no currently active sites over the Tropics; observations from the Nauru and Manus Tropical Western Pacific sites have been inactive since July 2014. The identification of candidate sites for expansion including consideration of existing GCOS Upper Air Network (GUAN) sites, for example in South America, Africa, Antarctica and the Tropics, was discussed following recommendations from the GRUAN expansion workshop held in June 2012 (Bodeker et.al, 2014). Although critical to the ultimate success of GRUAN, network expansion remains a challenge given the limited national resources for establishment of GRUAN sites.

However, ongoing coordination among GRUAN, NOAA and U.S. Department of Energy (DOE) Atmospheric Radiation Measurement (ARM) programs are effectively adding sites and RS92 radiosondes synchronized with NOAA Suomi-National Polar-orbiting Partnership (S-NPP) satellite overpass with further plans to synchronize with available Global Navigation Satellite System Radio Occultation (GNSS-RO) observations. Synchronized radiosonde and satellite measurements provide valuable datasets to monitor and inter-calibrate satellite sensors and associated Radiative Transfer (RT) models with feedback to GRUAN to identify possible in-homogeneities in data products across the network. Collocations of satellite and GRUAN processed radiosonde observations as routinely compiled and archived by the NOAA Products Validation System (NPROVS+) operated at the NOAA/NESDIS Center for Satellite Applications and Research (STAR), particularly those synchronized with satellite overpass, potentially have a high value for the Global Space-based Inter-Calibration System (GSICS). Further collaborations with the European Union (EU) Gap Analysis for Integrated Atmospheric Climate Monitoring (GAIA-CLIM) project (www.gaia-clim.eu) will also address issues such as ancillary data streams, collocation mismatch, data assimilation and inter-comparisons among measurements and products.

As with all GRUAN ICM meetings, a field trip to the local GRUAN site provided attendees an overview of the most vital aspect of GRUAN, namely, taking reference measurements. This year featured a balloon launch carrying a RS92 RAOB and an Ozonesonde from the Boulder GRUAN site courtesy Dr Dale Hurst (CIRES/ESRL). This site also launches monthly NOAA Frost-Point Hygrometers (FPH) but meteorological conditions precluded a water vapor sounding during the visit. Water vapor measurements, particularly in the upper troposphere and lower stratosphere (UTLS) provide important basis for satellite validation and are of great interest to climate scientists. Relatively significant

Return to Page 1

differences exist among the moisture burdens characterized by satellites, RAOBs and climate models that need to be reconciled. Increased FPH and/or Cryogenic Frost-point Hygrometers (CFH) launches at GRUAN sites (including at times of satellite overpass) are planned funding permitting.

In summary, the GRUAN ICM-8 provided five information-packed days on the status and activities surrounding the GRUAN program, strengths, weaknesses and the path forward. GRUAN is vibrant, growing and is expected to provide pivotal climate datasets useful for calibration and assessment consistent with WMO Integrated Global Observing System (WIGOS) strategic plans for climate and weather.

GRUAN ICM-9 is scheduled 12-16 June 2017, Helsinki, Finland.

References:

Bodeker, G.E., et.al, 2016: Reference Upper Air Observations for Climate: From Concept to Reality. *BAMS*, Vol. 97, No. 1,
DOI: http://dx.doi.org/10.1175/BAMS-D-14-00072.1

Bodeker, G., et.al, 2014: GRUAN report 4: Outcomes of the GRUAN Network Expansion Workshop, 60pp, http://www.dwd.de/EN/research/international_programme/gruan/download/gruan_rp-4.pdf?__blob=publicationFile&v=4

Immler F.J., et.al, 2010: Reference Quality Upper Air Measurements: Guidance for developing GRUAN data products. *Atmos. Meas. Tech.*, **3**, 1217-1231, doi:10.519/amt-3-1217

Discuss the Article

Announcements

Registration Opens for GSICS Users Workshop, 2016

By Lawrence E. Flynn(GCC Director), NOAA

Registration for the GSICS Users Workshop, 2016 has opened. One can register online at http://www.star.nesdis.noaa.gov/star/meeting_2016JPSSAnnual.php. As indicated in the last issue of the Newsletter, the GSICS Users Workshop, 2016 would be organized on 11 August 2016 as part of the Annual JPSS meeting at NOAA, College Park, MD, USA. The main aim of the Workshop would be to connect Producers (Current and future) of the GSICS products with the users of their products.

Unlike previous years, this year the GSICS Users Workshop has four sessions, each of 90 Minutes and spans the entire day. Members of the Satellite Calibration Community GSICS Members are especially encouraged to submit abstracts for Oral and Poster presentations to Manik Bali (mailto:Manik.Bali@noaa.gov).

Jérôme Lafeuille Bids Adieu to GSICS

By Manik Bali, NOAA

The GSICS Executive Panel Meeting (EP-17) in Biot, France organized on 2-3 June 2016 was the last GSICS event attended by Jérôme Lafeuille, who will retire from WMO on 30 June 2016

Jérôme joined the WMO secretariat in 2005 where he was the Chief of the Space-based Observing System Division until December 2015 , and continued until June 2016 as Senior Scientific Officer. Already a member of the early CGMS Task Force that laid down the foundation of GSICS in March 2006, he has always represented WMO in the GSICS executive Panel, GRWG and GDWG since the establishment of those bodies. During the last 11 years, Jérôme's contributions were vital to assist the Executive Panel Chairs and vice-chairs, initially Mitch Goldberg and now Peng Zhang and Ken Holmlund, in bringing together GSICS members, defining and publicizing the high-level goals of GSICS and shaping the Vision of GSICS for the coming decade.

Jérôme participated in a number of GRWG and GDWG meetings, providing valuable help in the two-way

communication between these working groups and the EP. He played a key role in defining the Terms of Reference of these groups and worked with the

GDWG and GRWG Chairs and the GCC to ensure consistency between the progress of scientific and technical activities and the strategic level of the Executive Panel. With Aleksander Jelenak he prompted in the adaptation of WMO Metadata (ISO 19115), the development of Filenaming conventions, and the definition of a GSICS catalogue. He designed and operated the GSICS portal (gsics.wmo.int). In 2009, with Bob Iacovazzi he attended the QA4EO Implementation Workshop where Bob presented the GPPA which has become a benchmark of application of QA4EO maturity on Earth Observation. In 2014, along with Tim Hewison, he presented GSICS to the CEOS WGCV meeting in Frascati to start formalizing the collaboration between GSICS and WGCV. As the initiator of OSCAR/Space, a powerful WMO resource on space-based instruments, he worked with the GDWG to link OSCAR with calibration information and event logs, or pre-launch instrument characterization.

Recently, Jérôme strived to seek recognition of GSICS as a component of the WMO Integrated Global Observing System (WIGOS) and of its contribution to the Architecture for Climate Monitoring from Space, highlighting the need for a high-level communication on what GSICS is, how it works, what it actually delivers (e.g. , initiating the development of a Guide to GSICS) and the benefits it generates to satellite users and operators. In serving GSICS as WMO representative and Secretary of the Executive Panel, Jérôme has been keen to maintain a consensus in the GSICS community while ensuring consistency with the forward-looking vision. His efforts will benefit to GSICS for many years to come and so will the friendships he has created over the years in the GSICS community.

We wish to thank Jérôme for the contribution he has made to GSICS and wish him well for the next phase of his life.

Discuss the Article

7th Asia/Oceania Meteorological Satellite Users Conference (AOMSUC-7) to be held in Incheon, Korea, 24-28 Oct 2016

By Doheyong Kim, KMA

This year the 7th Asia Oceania Meteorological Satellite Users Conference (AOMSUC-7) will be joined with two other conferences namely the 2nd AMS-Asia and 2nd KMA International Meteorological Satellite Conference. It will be held from 24-28 October 2016 in Incheon, Korea. The conference will cover several topics including those relevant to GSICS. These topics include

- Current and future meteorological satellite programs
- Geo-KOMPSAT-2A related status and application
- New development of applications and innovative methods of processing, combining, assimilating and blending/fusing satellite data
- Satellite data calibration/validation and climate/environmental monitoring [GSICS and ECV(Essential Climate Variables)]
- Atmospheric parameters derived from satellite observations
- Application of satellite data to data assimilation and numerical weather prediction(NWP)
- Application of satellite data to weather analysis, disaster monitoring (Water and energy cycle), nowcasting and forecasting
- Land surface and ocean parameters derived from satellite observations
- Space-based space weather measurements, analyses and prediction models
- Facilitation of data access and utilization [International sharing of software tools, documents, algorithms, and best practices]
- Capacity building and training activities [coordination/interaction of satellite testbeds/proving grounds, and joint development of new satellite products, satellite training and education, services and dissemination]

The abstract submission deadline is 31 Aug 2016. For details please visit the website http://nmsc.kma.go.kr/aomsuc7/announcement.jsp

GSICS-Related Publications

Ahn, H., D. Shin, J. Kim, and C. Choi. 2015. “Radiometric Calibration of the KOMPSAT-3.” In http://acrs2015.ccgeo.info/proceedings/THP3-63.pdf

B. R. Scarino *et al*., "A Web-Based Tool for Calculating Spectral Band Difference Adjustment Factors Derived From SCIAMACHY Hyperspectral Data," in *IEEE Transactions on Geoscience and Remote Sensing*, vol. 54, no. 5, pp. 2529-2542, May 2016. doi: 10.1109/TGRS.2015.2502904

Doelling, D.R., M. Sun, L.T. Nguyen, M.L. Nordeen, C.O. Haney, D.F. Keyes, and P.E. Mlynczak. 2016. “Advances in Geostationary-Derived Longwave Fluxes for the CERES Synoptic (SYN1deg) Product.” Journal of Atmospheric and Oceanic Technology 33 (3): 503–21. doi:10.1175/JTECH-D-15-0147.1.

Tobin, D., R. Holz, F. Nagle, and H. Revercomb (2016), Characterization of the Climate Absolute Radiance and Refractivity Observatory (CLARREO) ability to serve as an infrared satellite intercalibration reference, J. Geophys. Res. Atmos., 121, doi:10.1002/2016JD024770.

Li, Y.; Wu, A.; Xiong, X. Inter-Comparison of S-NPP VIIRS and Aqua MODIS Thermal Emissive Bands Using Hyperspectral Infrared Sounder Measurements as a Transfer Reference. *Remote Sens.* **2016**, *8*, 72. doi:10.3390/rs8010072

Gao, C.; Zhao, Y.; Li, C.; Ma, L.; Wang, N.; Qian, Y.; Ren, L. An Investigation of a Novel Cross-Calibration Method of FY-3C/VIRR against NPP/VIIRS in the Dunhuang Test Site. *Remote Sens.* **2016**, *8*, 77.

Submitting Articles to GSICS Quarterly Newsletter:

The GSICS Quarterly Press Crew is looking for short articles (~800 to 900 words with one or two key, simple illustrations), especially related to calibration and validation capabilities and how they have been used to positively impact weather and climate products. Unsolicited articles are received for consideration anytime, and if accepted, will be published in the next available newsletter issue after approval/editing. Note the upcoming spring issue will be a general issue. Please send articles to manik.bali@noaa.gov.

With help from our friends:

The GSICS Quarterly Editorial team would like to thank Dr. Laury Miller for the lead article in this issue. Thanks are also due to ChangYong Cao (NOAA), Taeyoung (Jason) Choi (NOAA), Tim Hewison (EUMETSAT), Ralph R. Ferraro (NOAA) and Lawrence Flynn (NOAA) for reviewing the articles in this issue.

Published By
GSICS Coordination Center
NOAA/NESDIS/STAR
NOAA Center for Weather and Climate Prediction,
5830 University Research Court
College Park, MD 20740, USA